Stratigraphic constraints for Miocene-age vertical motion along the Santa Clara fault, Espanola Basin, north-central New Mexico

Koning, Daniel, J., Sean D. Connell, Janet L. Slate, and Elmira Wan

2007, pp. 225-238. https://doi.org/10.56577/FFC-58.225

in:

Geology of the Jemez Region II, Kues, Barry S., Kelley, Shari A., Lueth, Virgil W.; [eds.], New Mexico Geological Society 58 th Annual Fall Field Conference Guidebook, 499 p. https://doi.org/10.56577/FFC-58

This page is intentionally left blank to maintain order of facing pages.

New Mexico Geological Society Guidebook, 58th Field Conference, Geology of the Jemez Mountains Region II, 2007, p. 225-238.

STRATIGRAPHIC CONSTRAINTS FOR MIOCENE-AGE VERTICAL MOTION ALONG THE SANTA CLARA FAULT, ESPAÑOLA BASIN, NORTH-CENTRAL NEW MEXICO

DANIEL J. KONING[1], SEAN D. CONNELL[2], JANET L. SLATE[3], AND ELMIRA WAN[4]
[1] New Mexico Bureau of Geology and Mineral Resources, 801 Leroy Place, Socorro, NM 87801; dkoning@nmt.edu
[2] New Mexico Bureau of Geology and Mineral Resources, 2808 Central Ave. SE, Albuquerque, NM 87106
[3]U.S. Geological Survey, P.O. Box 25046, Federal Center, Mail Stop 913, Lakewood, CO 80225
[4]U.S. Geological Survey 345 Middlefield Road, MS 975, Menlo Park, CA 94025

ABSTRACT — We examine the middle to late Miocene tectonic history of the Santa Clara fault (SCF) in the Española Basin, north-central Rio Grande rift. A part of the Embudo fault system, the northeast-trending SCF transfers strain between the San Luis and Española Basins. This fault dips to the southeast and exhibits a normal, east-down sense of offset and significant left-lateral slip. Comparing thickness changes of dated stratigraphic intervals across the SCF allows us to document the development of this structure during middle and late Miocene time. Our thickness comparisons indicate an increase in fault activity at ca. 12.7 Ma and suggest a prior increase in fault activity between 15 and 13 Ma. Between 11 and 10 Ma, the southward-flowing river associated with the Cejita Member (Chamita Formation) lapped westward 3 km onto the Santa Clara footwall, suggesting diminished subsidence during that time or increased sediment supply to this river. Approximately 430-500 m of stratigraphic separation of post-10 Ma Chamita Formation strata and lesser vertical offset of the Pliocene Puye Formation indicates that significant vertical motion along the SCF occurred after 10 Ma.

INTRODUCTION

This report examines the middle to late Miocene tectonic history of the Santa Clara fault (SCF) of the Embudo fault system, an important intrabasinal fault in the northern Española Basin. The SCF stretches a distance of 20 km between its northern end immediately east of the southern tip of Black Mesa and its southern end at Santa Clara Canyon (Fig. 1). This northeast-trending fault bends at its southern end and projects south towards the Pajarito fault system (Fig. 1).

The left-oblique Embudo fault system, which includes the Santa Clara, La Mesita, and Velarde faults in addition to faults in the southern San Luis Basin, collectively act as a transfer structure in accommodating extension between the Española Basin and the adjoining San Luis Basin to the north (Fig. 1; Muehlberger, 1979; Steinpress, 1980, 1981; Kelson et al., unpubl. report for the U.S. Geological Survey, 1997; Kelson et al., 2004). The San Luis Basin is an east-tilted half-graben. The eastern Española Basin consists of a half-graben tilted westward against two linked faults: the north-trending Pajarito fault system to the south and the northeast-trending SCF west of Española (Fig. 1; Koning et al., 2005b). Northeast of Española, strata mostly dip northwest towards the southeast-down SCF and the northwest-down, left-oblique Velarde fault. South of a local Bouguer gravity saddle and inferred anticline near the lower Rio Chama (Koning and Manley, 2003) lies a Bouguer gravity low on the immediate hanging-wall of the SCF, called the Santa Clara graben by Koning et al. (2004a). Under Black Mesa, strata are tilted eastward along the Velarde fault in the Velarde intrabasinal graben (Ferguson et al., 1995; Koning et al., 2004a). We thus consider these three faults as master faults because, in a regional sense, strata are tilted towards them both inside and outside of the intrabasinal grabens.

The siliciclastic sediment and volcanic rocks that fill the Rio Grande rift are called the Santa Fe Group (Spiegel and Baldwin,

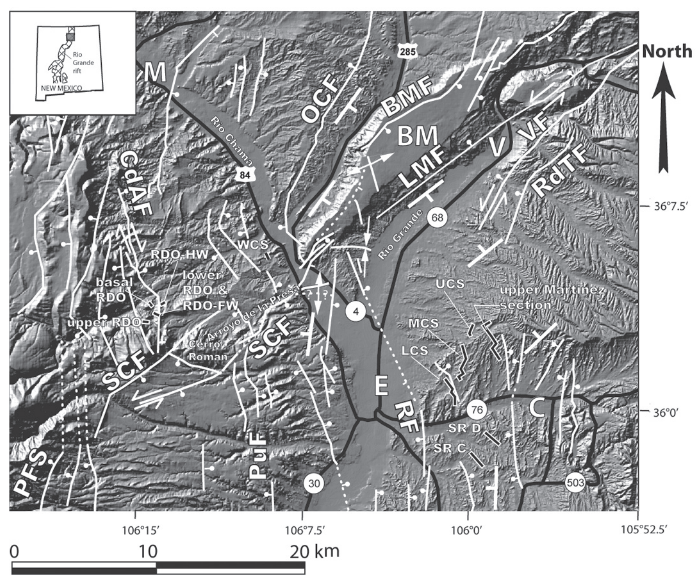

FIGURE 1. Shaded relief map showing locations of stratigraphic sections (thick black lines outlined in white): SR = Skull Ridge, UCS = upper Cuarteles section, MCS = middle Cuarteles section, LCS = lower Cuarteles section, RDO = Rio del Oso sections, WCS = West Chili section. Also depicted are faults (white lines, with ball and bar on the downthrown side) and folds (white lines = fold axis, with outward pointing arrows denoting anticlines and inward pointing arrows denoting synclines); dotted lines mark buried structures. Towns and other geographic features are abbreviated as follows: BM = Black Mesa, C = Chimayo, E = Española, V = Velarde, M = Medanales. Important faults are labeled as follows: OCF = Ojo Caliente fault, SCF = Santa Clara fault, BMF = Black Mesa fault, LMF = La Mesita fault, VF = Velarde fault, RdTF = Rio de Truchas fault, PuF = Puye fault zone, and PFS = Pajarito fault system. Fault locations and generalized dip directions are from Koning (2002, 2003, 2004), Koning et al. (2002, 2004c, 2005a), Koning and Manley (2003), and Koning and Aby (2003).

1963). In the Española Basin, the Santa Fe Group is subdivided into the Chamita Formation and the underlying Tesuque Formation. On the hanging wall of the SCF, previous studies suggested that the basin-fill sediments of the Santa Fe Group are 2.2-5.0 km thick (Kelley, 1978; Cordell, 1979; Koning and Aby, 2003; Koning and Manley, 2003). However, there is only about 1 km of basin-fill on most of the footwall of the fault (Baldridge et al., 1994; Koning et al., 2004a), indicating that 1-4 km of cumulative throw may have occurred on the SCF. The relatively shallow bench in the rift northwest of the SCF is known as the Abiquiu embayment (Kelley, 1978). Geophysical data (Baldridge et al., 1994; Koning et al., 2004a) and bedding attitudes (Kelley, 1978; Koning, 2004; Koning et al., 2004c) indicate that most of this bench is not tilted to the west, as is the eastern half-graben of the Española Basin (see minipaper by Koning et al., 2007). The western margin of the Abiquiu embayment coincides with a 17 km-wide zone of prominent east-down normal faults near Abiquiu. North of the Jemez volcanic field, these faults are interpreted to have served as the rift boundary until the late Miocene, when activity shifted eastward to the Pajarito fault and SCF (Baldridge et al., 1994).

Understanding the tectonic history of the SCF is important because it functions in part as a basin master fault for the west-tilted half-graben in the eastern Española Basin. Presumably, the tilting of that half-graben corresponds with motion along this fault.

PREVIOUS WORK

Early workers postulated that two phases of deformation affected the Española Basin. The first phase was marked by faulting and broad down-warping of the basin floor in the Oligocene-middle Miocene (Galusha and Blick, 1971; Baltz, 1978). The second phase formed the Española Basin proper and the high relief of the Sangre de Cristo Mountains, and was accompanied by faulting and tilting of the basin-fill strata from the late Miocene into the Pleistocene (Galusha and Blick, 1971), with only minor faulting in the Miocene (Kelley, 1978, 1979).

The above paradigm underwent a shift after 1978. Manley (1979) acknowledged faulting along the western rift border after ~10 Ma, but interpreted the inner grabens within the Española Basin as largely of Pliocene age. Golombek (1983) interpreted major tilting and faulting that initiated about 7.5 Ma, and argued that the Pajarito fault zone postdates 5 Ma.

Particularly germane are studies that interpret pre-10 Ma faulting near the study area. Baldridge et al. (1994) suggested that extension and significant faulting in the western Española Basin began around 10 Ma. Aldrich and Dethier (1990) interpreted predominantly dip-slip along the SCF from before approximately 12.4 to 10 Ma, predominantly oblique-sinistral strike-slip motion between 10 and 5 Ma, and dextral strike-slip thereafter. Dethier and Martin (1984) recognized that major extension occurred on the north flank of the Jemez Mountains between about 12 and 9.5 Ma. Koning et al. (2004a) used seismic reflection data to suggest that the Velarde graben began forming sometime between late Oligocene to late Miocene time, and Koning et al. (2005b) interpret middle Miocene tilting east of Española.

SANTA CLARA FAULT

Santa Clara fault (SCF) was the first name applied to this structure (Harrington and Aldrich, 1984). Many subsequent workers (e.g., Aldrich, 1986; Aldrich and Dethier, 1991; Gonzalez, 1993; Machette et al., 1998) used the name Embudo fault because the fault strikes northeast like the La Mesita fault of the Embudo fault system. Earlier maps (e.g., Kelley, 1978) portrayed the two faults as a continuous structure. However, recent work indicates that the two structures are not continuous, at least near the surface, but rather undergo a structurally complicated right step at and east of the south tip of Black Mesa, called the Black Mesa segment boundary (Koning et al., 2004a). Furthermore, the sense of throw (northwest-down on the northern faults versus southeast-down on the SCF) reverses in this step-over. We feel it is justified to use a separate name when referring to this fault, and other workers have recently readopted the name SCF as well.

The SCF is marked by a relatively wide zone (hundreds of meters) of steeply southeast-dipping beds of the Chamita Formation (30° to vertical, some overturned). Within this zone are one or more northeast-striking faults. On the south side of Arroyo de la Presa, the strike of the fault zone has a zigzag pattern (Figs. 1, 2), alternating between easterly strikes of about N70-80°E and northerly strikes of N30-40°E. Slickenside data on the more northerly striking sections indicate a left-lateral sense of motion (Gonzalez, 1993). Aldrich (1986) and Aldrich and Dethier (1991) interpreted a significant component of strike-slip along this fault based on the orientation of conjugate shears, and inferred a right-lateral direction because north-northeast sections of the fault showed signs of compression or transpression and lacked adjoining pull-apart basins. However, we suspect a general left-lateral component of slip based on the following: 1) at one locality, measurements on a N70-80°E striking section of the fault indicate a sinistral-oblique sense of fault motion (D. Koning, unpubl. data; UTM coordinates: 397339 E, 3991446N, NAD 27, zone 13); 2) on an easterly striking section of the fault about 0.5 km northeast of the aforementioned locality, beds that strike roughly parallel to the fault are locally overturned (Koning et al., 2005a), indicating transpression along this easterly striking segment consistent with sinistral slip along the generally northeast striking faults, and 3) Lobato Formation basalt flows 2-3 km north of the fault near the town of Chili are generally rotated counter-clockwise (Brown and Golombek, 1985; Salyards et al., 1994).

The magnitude of lateral slip is not known for the SCF, but the cross-section shown in figure 1.18 of the first day road log (also in Koning and Manley, 2003; Koning et al., 2005b) suggests a late Miocene-to-present throw of 430-500 m. This throw estimate uses the stratigraphic separation of a phreatomagmatic deposit encountered in the Agua Sana South Well #1 that may correlate with exposed, 12-25 m-thick, phreatomagmatic deposits underlying Lobato Formation basalt flows on the fault footwall. The base of these flows returned a K/Ar age of 12.4 ± 0.4 Ma (Dethier et al., 1986; Aldrich and Dethier, 1990) and a preliminary $^{40}Ar/^{39}Ar$ age of 9.54 ± 0.66 Ma; a bomb in the underlying, thick phreatomagmatic deposits returned a preliminary age of 9.0 ± 1.4 Ma (Richard Esser, written commun., 2006).

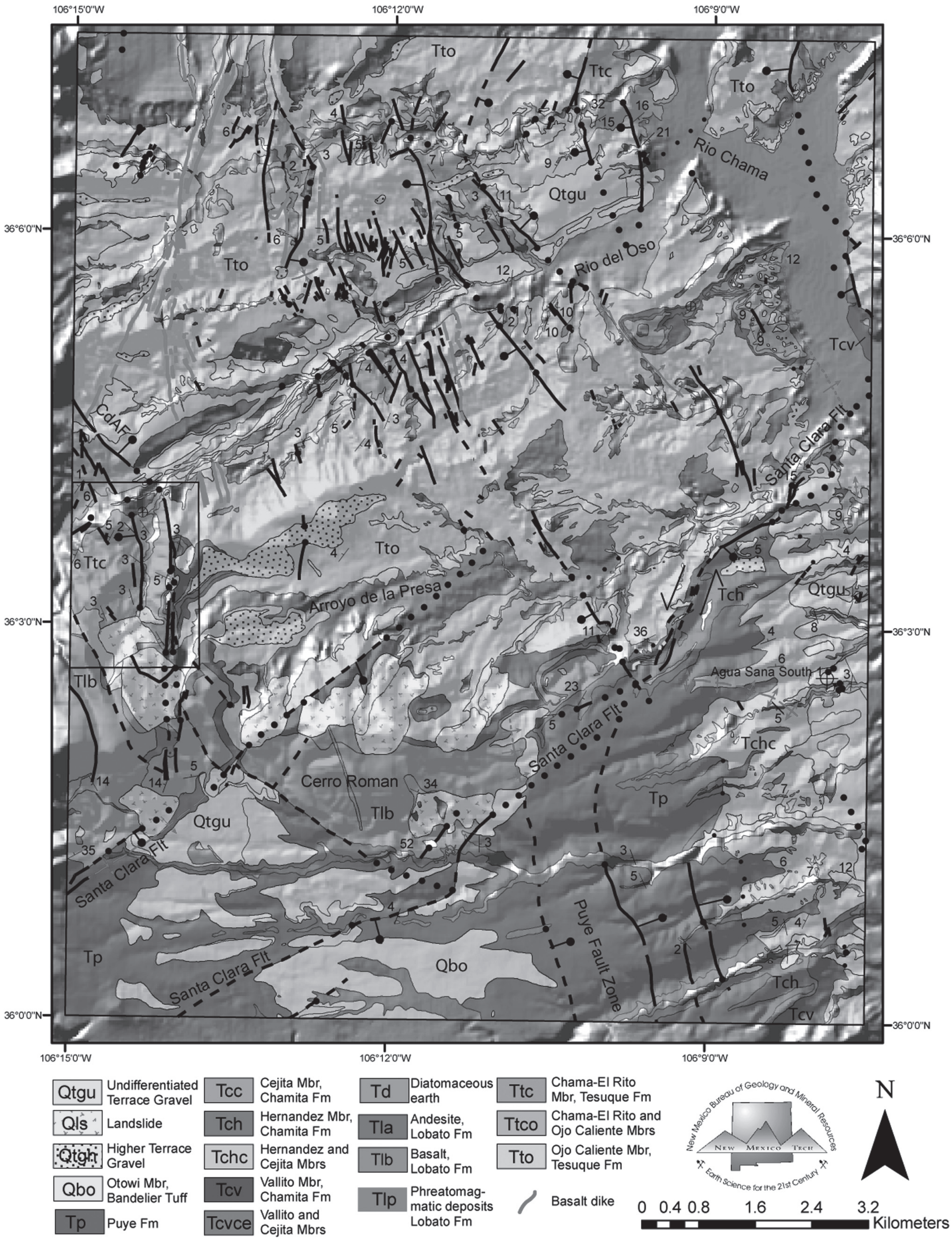

FIGURE 2. Geologic map of the Chili 7.5-minute quadrangle (Koning et al., 2005a). Rectangular box along west margin is location of map of figure 1.73 of 1st-day road log. CdAF = Canada del Almagre fault. Quaternary valley-fill units not shown. For color version of this figure, see Plate 10 on page 140.

Three to four km east of Cerro Roman, the trace of the SCF becomes somewhat enigmatic in the poorly exposed Puye Formation (Fig. 1). Here, the north end of the Puye fault zone projects into the SCF (Figs. 1, 2). We suspect that a component of slip is transferred between the Santa Clara and Puyé faults in this area. Near Cerro Roman is a 2-3 km right-step in the SCF. The northern, northeast-striking fault in this step-over joins with the north-striking Pajarito fault near Santa Clara Canyon to the south and has formed a prominent scarp on the western edge of the Pajarito plateau. The southern fault is marked by a degraded fault scarp in the Puye Formation approximately 18 to 32 m high.

METHODS

We compare stratal thicknesses between the footwall and the hanging wall of the SCF. If no motion on the fault occurred during deposition of a particular stratigraphic interval, then the thickness of that interval should be similar on both sides of the fault, assuming no relict topography (of which there is no evidence in our study sites). If the hanging wall of the fault was subsiding, then the hanging-wall succession should be thicker than on the footwall, owing to the difference in accommodation and preservation of sediment. Thickness differences may be even more pronounced if the footwall block was subject to erosion. Other variables that may influence stratal preservation and sedimentation, such as discharge or paleoclimatic variations, are assumed to apply more or less equally on both the hanging wall and footwall. Ideally, the streams associated with the deposits should be approximately similar in size because smaller tributary streams may have steeper gradients and somewhat thinner deposits than larger, higher order streams.

Stratal thicknesses are compared between specific tephra beds or zones that we can correlate between stratigraphic sections in the footwall and hanging wall. Other faults between the hanging-wall stratigraphic sections and the SCF may also influence stratal thicknesses, but they are inferred to be relatively minor compared to the SCF (e.g., fig. 1.18 of the 1st day road log). Of these faults, the one having the most throw is located ~3.7 km east of the SCF (120-150 m east-down throw vs. >430-500 m on the SCF). Another relatively long structure, the Road fault east of Española, has an interpreted throw of 18 m (Johnpeer et al., 1985) north of NM-76. Activity along these intermediary faults may influence the thickness differences, but probably to a lesser degree than motion along the SCF. Another potential complication is thickness variations due to sinistral motion of different parts of the basin. We think this is not significant because Bouguer gravity contour lines in the immediate areas of our footwall and hanging-wall sites are generally parallel to the strike of the SCF (Ferguson et al., 1995). In other words, basin-fill strata seem to be of relatively constant thickness parallel to the fault, so movement along the fault probably would not juxtapose areas that may have experienced different subsidence rates (and hence thicker basin-fill).

Below, we summarize our stratigraphic sections and the tephra marker beds or zones. We conclude with a comparison of thickness changes between sections and discuss how the activity and motion along the SCF changed during the middle and late Miocene.

STRATIGRAPHY

Stratigraphy near the SCF

As an introduction to our stratigraphic sections, we summarize the stratigraphy on the footwall and hanging wall of the SCF (Fig. 3). Strata on the footwall generally consist of two sandy members of the Tesuque Formation, the fluviatile Chama-El Rito Member (1000-2000(?) m thick) and the overlying, predominately cross-stratified, eolian sediment of the Ojo Caliente Sandstone Member (180-360 m thick). These two members have interpreted age ranges of 18(?) to 13.4 Ma and 13.4 to 12.5 Ma, respectively (May, 1980, 1984; Ekas et al., 1984; Dethier et al., 1986; Aldrich and Dethier, 1990; Tedford and Barghoorn, 1993; Tedford et al., 2004; Koning et al., 2005a, b).

Locally on top of the Tesuque Formation lies the relatively thin (40-100 m) Chamita Formation, which consists of sand, silty sand, gravel, and clay-silt beds that belong to the Vallito, Hernandez, and Cejita Members. The Hernandez Member consists of pebbly sand and sandy gravel channel-fills along with floodplain deposits of an ancestral Rio Chama. To the northeast, the Hernandez Member interfingers with the Vallito and Cejita Members. The Vallito Member consists of sandy ancestral Rio Grande deposits derived from the San Luis Basin (Koning and Aby, 2005) and interfingering, distal alluvial slope deposits of streams with a source in the Abiquiu embayment. The Cejita Member consists of floodplain sediment and sand to pebbly sand channel-fills deposited by a river draining the Peñasco embayment to the northeast (Manley, 1976, 1977, 1979; Koning and Aby, 2005). This river merged with the one draining the San Luis Basin immediately north of our study area, and Cejita Member sediment input dominates the axial river deposits on the SCF footwall. Depending on location, the contact between the Chamita and Tesuque Formations may be either unconformable or gradational.

Intercalated with and generally overlying the Chamita Formation on the SCF footwall are basalt flows of the Lobato Formation. At Cerro Roman, stacked flows attain a cumulative thickness as much as 180 m (Koning et al., 2005a). K/Ar age ranges of basalts in the vicinity are 12.4 ± 0.4 Ma to 9.6 ± 0.2 Ma (Dethier and Manley, 1985; Dethier et al., 1986; Goff et al., 1989), mostly between 11-9.5 Ma, and a recent $^{40}Ar/^{39}Ar$ date returned an age of 9.82±0.28 Ma (Justet, 2003). Also of significance is the Rio del Oso dike swarm, which consists of subvertical basalt dikes that intrude the Ojo Caliente Sandstone and Chama-El Rito Members north of Arroyo de la Presa. These dikes have been dated at 10.7-9.3 Ma (Baldridge et al., 1980; Dethier et al., 1986; Aldrich and Dethier, 1990; Koning et al. 2005a), and indicate east-west extension during that time (Baldridge et al., 1980). More detail on the stratigraphy of the footwall can be found in Dethier and Martin (1984), Dethier and Manley (1986), and Koning et al. (2005a).

On the hanging wall of the SCF, the Tesuque Formation underlies the coarser-grained Chamita Formation. The exposed Tesuque Formation is formally subdivided into three members:

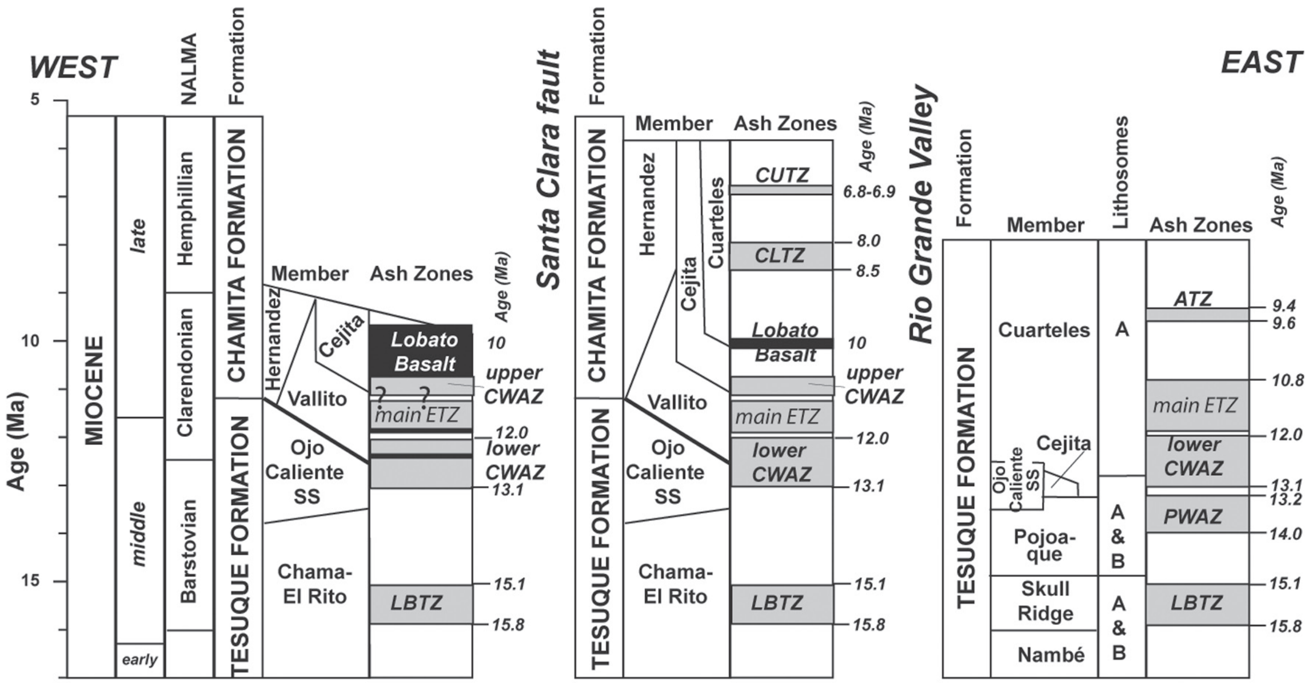

FIGURE 3. Schematic diagram illustrating age relations of middle to upper Miocene lithostratigraphic units and tephra of the north-central and northwestern Española Basin. Black rectangles represent Lobato Formation basalt flows. LBTZ = lower Barstovian tuffaceous zone, PWAZ = Pojoaque white ash zone, CWAZ = lower coarse white ash zone, ETZ = Española tephra zone, CLTZ = Chamita lower tuffaceous zone, and CUTZ = Chamita upper tuffaceous zone (latter two discussed in Koning et al., 2005b). NALMA = North American land mammal "age."

the Nambe, Skull Ridge, and Pojoaque Members (bottom to top; Galusha and Blick, 1971). Within these three members, Cavazza (1986) differentiated two interfingering lithosomes (A and B) that indicate two distinctly different provenances. Buried under Chamita Formation strata immediately adjacent to the SCF are the Ojo Caliente Sandstone and Chama-El Rito Members (Fig. 3). As a whole, strata become significantly coarser after ~13.2 Ma. These coarser, Miocene-age deposits have been formally designated as the Cejita Member for strata similar to lithosome B (Manley, 1976, 1977, 1979; Koning et al., 2005b) and as the Cuarteles Member for lithosome A strata (Koning et al., 2005b). Both these members extend across the Chamita and Tesuque Formations, as allowed by NACSN (2005). Further description of the sediments and the stratigraphy of hanging-wall strata was given by Koning and Aby (2005) and Koning et al. (2005b).

On the SCF footwall, we measured stratigraphic sections in two general areas (descriptive data in Koning et al., 2005a). Along the middle part of Rio del Oso, about 1 km east of the abandoned village of San Lorenzo, are five stratigraphic sections: the basal, lower, and upper Rio del Oso sections together with the hanging-wall Rio del Oso section (RDO-HW) and the footwall Rio del Oso section (RDO-FW) (Fig. 1; 1st day road log, fig. 1.72). The basal, lower, and upper Rio del Oso sections exhibit strata of the Chama-El Rito and basal Ojo Caliente Sandstone Members of the Tesuque Formation (Fig. 4). The RDO-HW and RDO-FW sections were mainly measured in Chamita Formation strata intercalated with Lobato Formation basalt flows (Fig. 5); they also indicate 13 to 10 Ma activity along the Cañada del Alamgre fault (see minipaper by Koning and Kempter, 2007). The base of RDO-HW corresponds with a gradational and possibly interfingering contact with the upper Ojo Caliente Sandstone, and the base of RDO-FW corresponds to an unconformity on the top of the Chama-El Rito Member (Fig. 5). The second area lies 1.4 km south-southwest of the town of Chili, where the West Chili stratigraphic section was measured in interfingering Vallito and Cejita Members of the Chamita Formation (Fig. 6). The base of this section is in the upper Ojo Caliente Sandstone Member.

These six stratigraphic sections document sedimentologic differences between the Chama-El Rito Member of the Tesuque Formation and the various members of the Chamita Formation. In the former, tephra consists of gray and white fine ash contained within discrete beds and paleosols are generally absent. In addition, sedimentary structures such as horizontal laminations, ripple marks, or cross-stratification are generally preserved within thin to medium, tabular to broadly lenticular sand beds.

In contrast, stratigraphic sections in the Chamita Formation locally exhibit abundant paleosols (e.g., West Chili section) and tephra consists of white coarse ash-fine lapilli that may be in discrete beds but is commonly diluted and scattered within sand, silty sand, and mud beds. Furthermore, sedimentary structures are generally lacking in sand beds of the Vallito Member (i.e., these beds are internally massive).

We compare stratal thicknesses in these footwall sections to previously measured stratigraphic sections east of Española in the hanging wall of the fault (Figs. 1, 7, 8). These sections include the Cuarteles and upper Martinez stratigraphic sections (Koning, 2003; Koning and Manley, 2003; Koning et al., 2005b). Located in the escarpment north of the Santa Cruz River, these sections

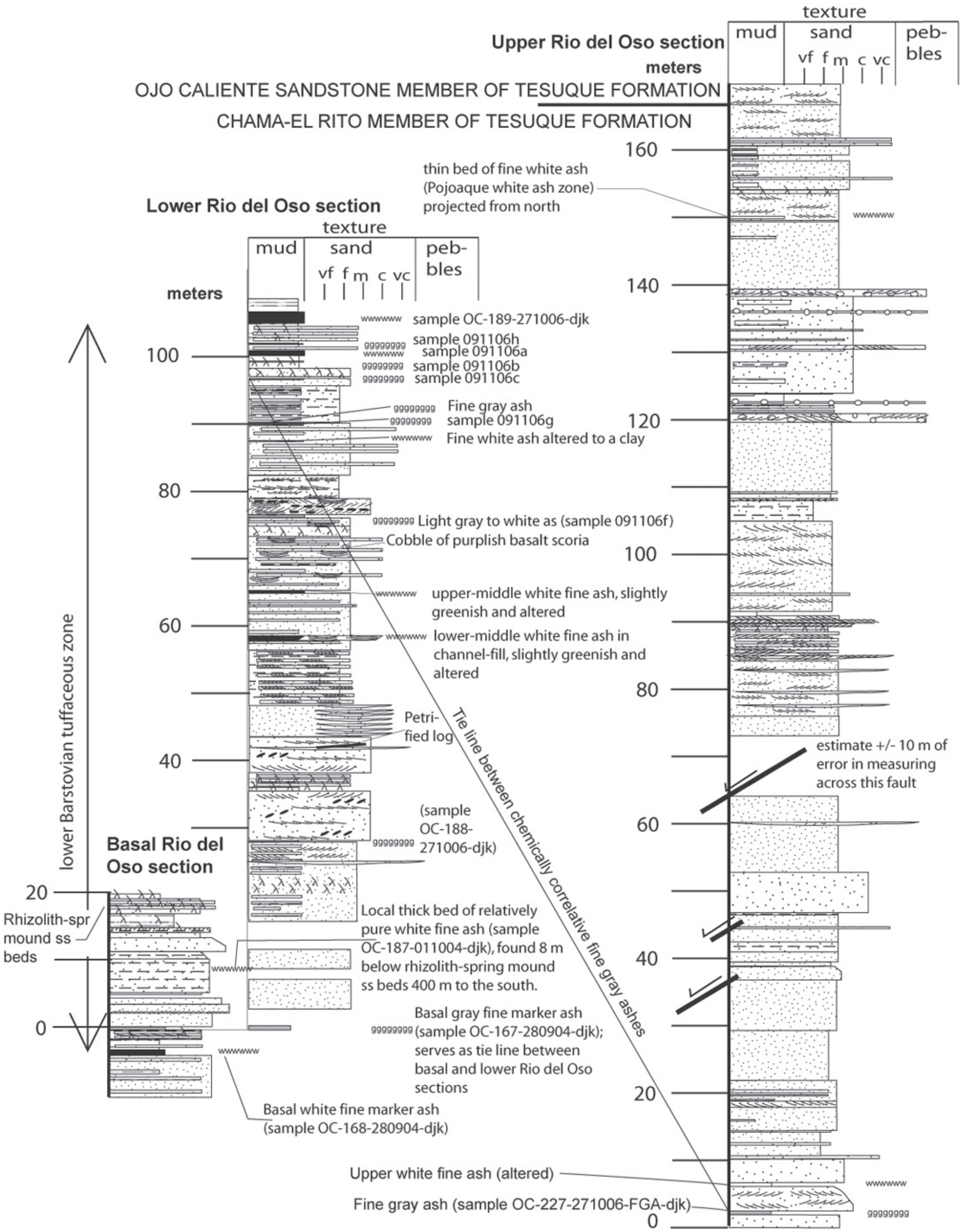

FIGURE 4. Rio del Oso sections that illustrate the ash-bearing Chama-El Rito (inferred lower Barstovian tuffaceous zone), overlying Chama-el Rito, and the basal Ojo Caliente Sandstone Members of the Tesuque Formation. Correlations between the basal, lower, and upper Rio del Oso sections are depicted. See Koning et al. (2005a, appendix) and 1st-day road log (fig. 1.73) for detailed descriptions and locations of these sections, and Figure 6 for explanation of stratigraphic section symbols and patterns.

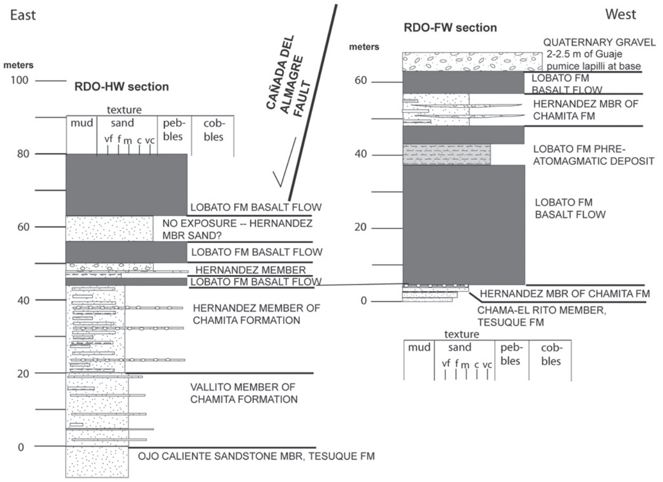

FIGURE 5. RDO-HW and RDO-FW stratigraphic sections illustrating the Chamita Formation and intercalated Lobato Formation basalts near the Rio del Oso stratigraphic sections. Sense of throw along the Cañada del Almagre fault is interpreted from juxtaposition of stratigraphic units found on either side of the fault, such as the younger Chamita Formation on the east side of the fault juxtaposed against the older Chama-El Rito Member of Tesuque Formation on the west side of the fault (Fig. 2; Dethier and Martin, 1984; Aldrich and Dethier, 1990; Koning et al., 2005a). See Koning et al. (2005a, appendix) and 1st-day road log (fig. 1.73) for detailed descriptions and locations of these sections, and Figure 6 for explanation of stratigraphic section symbols and patterns.

extend up-section from the upper Pojoaque Member into coarse strata of the Cuarteles Member of the Tesuque Formation (Fig. 8). We also use stratigraphic sections D and C from Kuhle (1997) to illustrate stratigraphic positions of tephra in the Skull Ridge Member (Tesuque Formation) between White ashes 2 and 4 (Figs 1, 7). These sections are extended upwards to the Pojoaque-Skull Ridge contact using map data and notes from Koning (2002), Koning et al. (2002), and Koning (unpubl. data).

Marker beds and zones

Five dated tephra beds or zones serve as boundaries of stratigraphic intervals whose thicknesses are compared across the Santa Clara fault (Table 1). The 9.4-10 Ma age datum consists of the basal Alcalde tuffaceous zone (ATZ, in the hanging wall) and a 3 m-thick basalt that caps the West Chili section in the footwall. The dark-colored, coarse ashes of the main Española tephra zone (ETZ) lie in a 24 m-thick interval 28-52 m above the lower coarse white ash zone. Because of their uniqueness within the ETZ, we correlate pumice-bearing beds of the 12.9-15.7 m interval in the West Chili stratigraphic section with the 397.0-410.6 m interval in the Cuarteles stratigraphic section of Koning, (2003) and Koning et al. (2005b).

Within the lower coarse white ash zone (LCWAZ), a particularly useful tephra for correlation purposes is a distinctive white coarse ash- lapilli bed consisting of a mixed assemblage of pumice and hetereolithic, angular, felsic-intermediate lapilli (up to 30 mm lomg) that includes a greenish, porphyritic dacite. We believe that the coarseness of this lapilli and the presence of the greenish dacite clasts are sufficiently distinct and unique to use for correlation purposes. In the Cuarteles section, this greenish dacite-bearing lapilli bed lies 2.5 m below a pumice-bearing tephra bed dated using $^{40}Ar/^{39}Ar$ at 12.71 ± 0.74 Ma, so we assign this lapilli bed an approximate age of 12.7 Ma as well. The entire LCWAZ has an age range of 13.1 to 12.1 Ma (Koning, 2007).

About 110 m below the LCWAZ on the hanging wall is the Pojoaque white ash zone in Pojoaque Member strata of the Tesuque Formation, having an age range of 13.2-14.0 Ma (Table 1; Koning et al., 2005b and references therein). On the footwall, geologic mapping in the Lyden and Chili quadrangles (Koning, 2004; Koning et al., 2005a) indicates that several white fine ashes occur in the basal 20-40 m of the Ojo Caliente Sandstone Member (including the gradational zone with the underlying Chama-El Rito Member) and upper 40-60 m of the Chama-El Rito Member. These ashes look similar to those in the Pojoaque white ash zone in the SCF hanging-wall (Table 1). Moreover, both sets of ashes occur in strata yielding fossils correlated with the late Barstovian North American land mammal "age" (Tedford and Barghoorn, 1993). Thus, we infer these two sets of white fine ashes corre-

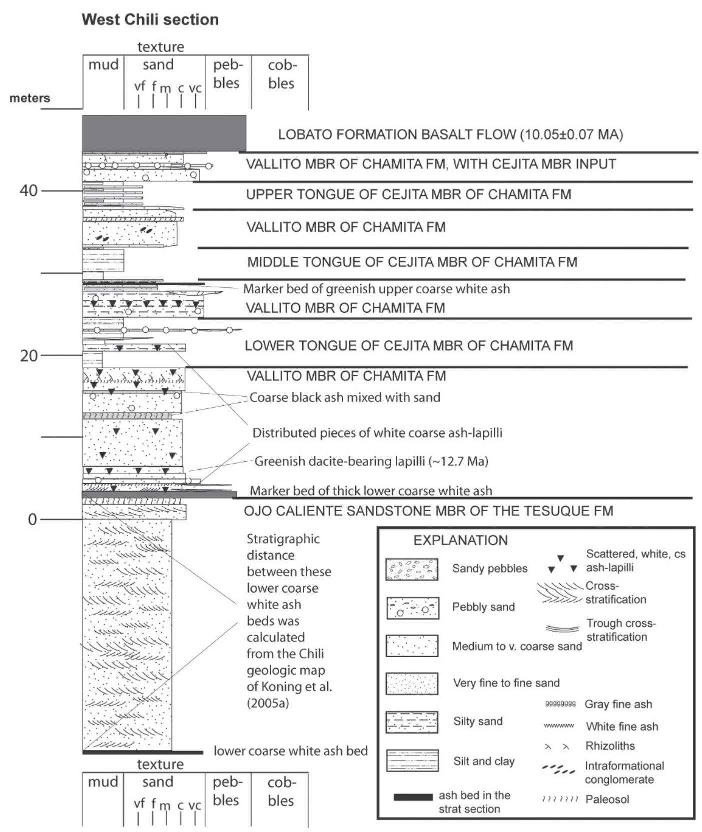

FIGURE 6. West Chili stratigraphic section. Upper Ojo Caliente Sandstone Member (Tesuque Formation) constitutes base of section; above lies interfingering Vallito and Cejita Members of the Chamita Formation. The Vallito Member here is interpreted as distal piedmont stream deposits that reworked the Ojo Caliente Sandstone Member in the Abiquiu embayment. Age of capping basalt is from Maldonado and Miggins (2007). UTM coordinates of the top andat 0 m of the section are 0396235 E, 3994500 N and 0396252 E, 3994420 N (zone 13, NAD 27). Lowest coarse white ash bed projected from 730 m to NE.

TABLE 1. Summary of tephra beds and zones

Tephra bed or zone *(source)*	Stratigraphic position on FW *(strat section)*	Stratigraphic position on HW *(strat section)*	Lithologic Summary and age*
9.4-10 Ma age datum *(Lobato Fm eruptive center)*	44.8-47.8 m *(West Chili)*	556.4-558.3 m (*Martinez)*	**Basal Alcalde tuffaceous zone on HW**: One to two, laterally extensive, thin to thick ash beds (9 to 12 m of stratigraphic separation m) that are black to gray, fine to coarse (mostly coarse), and are probably basaltic in composition. Top of ATZ is 9.40 ± 0.46 Ma (Koning et al., 2004b), so base ~50 m below is probably ~9.4-10 Ma. **Lobato Fm basalt flow on FW**: very dark gray; 10.11 ± 0.07 Ma (Maldonaldo and Miggins, this volume).
Main Espanola tephra zone *(buried vents near center of the Española Basin)*	12.3-15.7 m *(West Chili)*	386.8-410.6 m *(Cuarteles)* 453.6-476.4 m *(Martinez)*	**HW**: One to eight, black to dark gray to light gray, coarse ash beds intercalated in arkosic sandstone and granite-dominated, gravelly channel-fills. In unit 8p (410.6 m) and unit 8j (397.0-397.7 m) of the Cuarteles section are locally abundant, white consolidated ash and pumice (0.5 - 17 mm in diameter). Age estimate of 10.2 to 12.4 Ma. **FW**: 8-20% black-gray basalt-andesite grains mixed with sand composed of quartz + 10-12% orange-stained quartz and possible potassium feldspar; also 2-4 mm-long pumice grains and clasts; locally part of paleosols. At 12.9 m and 15.4-15.7 m in the W. Chili section are dark-colored, coarse ash beds that contain minor (~2-5%) white ash-pumice grains and clasts 0.5-4 mm in diameter. Age estimate of 10.2 to 12.4 Ma
Lower coarse white ash zone *(northern Jemez Mtns)*	Four beds between 0.8 and 12.3 m. Another bed projects 29 m below base of section *(West Chili)*	372.8-442.4 m *(Martinez)* 280.5-359.3 m *(Cuarteles)*	Thin to thick beds containing coarse ash- to lapilli-size fragments of compacted white ash, pumice, and plagioclase crystals together with 1-10% biotite, 3-7% pink to light gray, felsic-intermediate volcanic rock ejecta, 3-5% quartz, and trace to 2% hornblende. These are intercalated within arkosic sand and gravelly channel-fills (Cuarteles Mbr., Tesuque Formation) in the HW sections, and within sand and pebbly sand (Vallito and Hernandez Member) strata in the FW sections. Within this zone is a bed containing hetereolithic, felsic-intermediate lapilli (25-30 mm) that includes a greenish, porphyritic dacite. Age range of 12.1-13.1 Ma (Koning et al., minipaper, this volume); the greenish porphyritic dacite lies 2.5 m below a pumice-bearing bed having a $^{40}Ar/^{39}Ar$ age of 12.71 ± 0.74 Ma.
Pojoaque white ash zone *(western Nevada &Snake River Plain, ID)***	See text	73-170 m *(Cuarteles)*	Numerous, thin to thick, tabular beds of fine white and local gray ashes interbedded in sandstone, silty sandstone, and siltstone of lithosomes A and B of the Pojoaque Member of the Tesuque Formation. White ashes generally altered and contain very sparse to sparse glass shards and up to 7% biotite. Assigned age of 14.0 Ma and 13.2 Ma (Koning, 2003 using magnetic-polarity stratigraphy work of Barghoorn, 1981, the revised geomagnetic polarity time scale of Cande and Kent, 1995, and fossil data (Koning et al., 2005b; Tedford et al., 2004, Tedford and Barghoorn, 1993). $^{40}Ar/^{39}Ar$ age of 13.7 ± 0.18 Ma (Izett and Obradovich, 2001) obtained in the lower-middle part of the PWAZ (Obradovich, written commun, 2004) in the Pojoaque Member type section.
Lower Barstovian tephra zone[¥]	See text		Abundant white and gray, fine ashes in sandstone and siltstone of lithosomes A and B in the Skull Ridge Member of the Tesuque Formation.

Notes: HW = hanging-wall, FW = footwall

* Complete description of these tephra zones and their ages are given in Koning et al. (2005b), unless otherwise noted.

** Andrei Sarna-Wojcicki (unpublished data)

[¥] A large possibility of source areas, include Snake River Plains origin.

late with one another (i.e., are part of the PWAZ). One thin bed of altered fine white ash projects to 150 m in the upper Rio del Oso section. Since it lies only 17 m below the Ojo Caliente and Chama-El Rito Member contact, we correlate this ash to about the middle of the Pojoaque white ash zone.

One of the defining characteristics of the Skull Ridge Member of the Tesuque Formation is abundant white and gray, fine ash beds (Galusha and Blick, 1971; Koning et al., 2002). Our lower Rio del Oso section (Fig. 4) includes several ashes similar in appearance and abundance to those in the Skull Ridge Member. The ashes are not chemically similar to those in the Pojoaque white ash zone, the only other tephra zone with the same abundance of ashes. Correlating ashes in the lower Rio del Oso section with those in the Skull Ridge Member is consistent with suggestive biostratigraphic data. The Skull Ridge Member has yielded fossils belonging exclusively to the early Barstovian North American land mammal "age" (15-16 Ma; Tedford et al., 2004; Tedford and Barghoorn, 1993). Strata of the lower Rio del Oso section likely correlate to what Tedford and Barghoorn (1993, fig. 2) called the Rio del Oso-Abiquiu sites, which also yielded early Barstovian fossils. The only place we know of where early Barstovian fossils could possibly be collected along Rio del Oso is on the footwall of the Cañada del Almagre fault, because east of that fault Rio del Oso is generally within 60 m of the Chama-El Rito and Ojo Caliente contact (which would have yielded late Barstovian fossils according to Galusha and Blick, 1971, and Tedford and Barghoorn, 1993).

To test the suggestive biostratigraphic data regarding a correlation with the Skull Ridge Member, we analyzed the chemical compositions of all relatively unaltered ashes in the lower Rio del Oso section (Tables 2, 3). We then compared their compositions to two extensive, distinctive white ashes in the Skull Ridge Member on the hanging wall, called White ash #2 and White ash #3, using chemical composition data in Borchert (2002). Variables involved in comparing data sets from different labs make our resulting interpretations preliminary and inconclusive until we run them all on the same instrument. Initial results, however, are promising. Of the approximately 5500 entries in the USGS

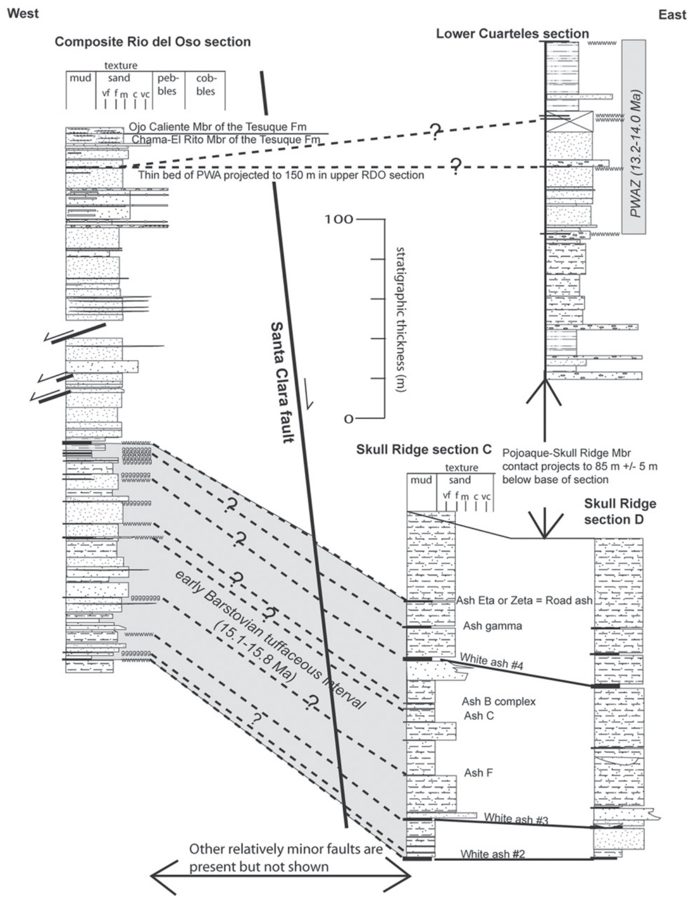

FIGURE 7. West-east stratigraphic fence diagram illustrating our correlations between middle Miocene footwall and hanging-wall strata relative to the SCF. The Skull Ridge sections C and D are slightly modified from Kuhle (1997) and Kuhle and Smith (2001) using Koning et al. (2002), Koning (2002), and unpubl. data of D. Koning.

tephrochronology database, sample OC-187, located 12 m above the basal white fine marker ash, chemically matches best with Skull Ridge White ash #3 (using our selected elements; Table 3 and Fig. 4).

At this stage in our study, it is useful to compare the thickness of the entire tuffaceous interval in the strata inferred to be ~15-16 Ma (early Barstovian) based on biostratigraphic data. The top and base of this informal lower Barstovian tuffaceous zone in the Skull Ridge Member correspond to the Road ash and White ash #2, respectively; White ash #2 may correlate with the basal white fine marker ash (Table 3; Fig. 7). Ashes are present above and below this tuffaceous zone, but are relatively sparse and widely spaced (Kuhle, 1997; Kuhle and Smith, 2001; Galusha and Blick, 1971). Near the Skull Ridge type section (near the C Skull Ridge section, Figs 1, 7), tephra are sufficiently abundant between these two ashes that they may be considered as a marker interval 160-180 m thick. The Road ash returned a $^{40}Ar/^{39}Ar$ age of 15.1 ± 0.06 Ma, and the age of White ash #2 is constrained by $^{40}Ar/^{39}Ar$ dating and magnetic-polarity stratigraphy work to range from 15.8 to 15.5 Ma (Barghoorn, 1981; Izett and Obradovich, 2001).

Ashes in this lower Barstovian tuffaceous zone that locally proved important are a gray fine ash near the top of the lower Rio del Oso section (sample 091106c) at 96.5-96.6 m, and another near the base of the upper Rio del Oso section (sample OC-277-271006-FGA-djk) at 2.1-2.5 m (Fig. 4). These two ashes are sufficiently similar in composition to justify correlation (Table 2). Correlating these ashes is consistent with projecting the contact between the two sections using local measurements of bedding attitudes (within the estimated ±15 m of error involved in such a projection). Thus, we are able to use the tephra composition data to confirm our tie between the lower and upper Rio del Oso stratigraphic sections.

STRATAL ACCUMULATION RATES

The abundant, relatively well-dated tephra markers in the Española Basin provide constraints for comparing stratal accumulation rates in the region (e.g., Koning et al., 2005b). We use some of these tephra to correlate strata across the SCF zone. We define four stratigraphic intervals: 1) 10-12.7 Ma interval between the 9.4-10 Ma age datum and the greenish dacite-bearing lapilli bed in the lower coarse white ash zone; 2) 12.7-13.1 Ma interval between the greenish dacite-bearing lapilli bed in the lower coarse white ash zone and the base of this zone; 3) 13.5-15.1 Ma interval between the middle of the PWAZ and the top of the lower Barstovian tuffaceous zone; and 4) 15.1-15.8 Ma interval corresponding to the lower Barstovian tuffaceous zone in Skull Ridge age-equivalent strata.

We compare the stratigraphic thicknesses of these four stratigraphic intervals across the SCF zone. A hanging wall-normalized thickening index, equal to the thickness difference between the hanging wall and footwall divided by the hanging wall thickness, is used to assess the amount of thickening of a particular stratigraphic interval across the SCF. Since we may be off ±10 m in our correlations (except for the greenish dacite-bearing lapilli), the estimated error involved in this calculation is about 15%. We also calculated stratal accumulation rates using our thickness and age data (Table 4).

These calculations indicate a progressive up-section increase in the hanging wall-normalized thickening index, from 16 to 22% in the lower Barstovian tuffaceous zone to 75% in the interval between the 9.4-10 Ma age datum and the greenish dacite-bearing lapilli bed. Stratal accumulation rates also decrease up-section in both the hanging wall and the footwall. However, the hanging wall-normalized thickening index and sedimentation rates are similar between the two middle stratigraphic intervals (i.e., between the top of the lower Barstovian tuffaceous zone and the greenish dacite-bearing lapilli bed). For each stratigraphic interval, the range of footwall sedimentation rates is generally lower than the range of hanging wall sedimentation rates.

DISCUSSION

Temporal changes in vertical motion along the SCF

Biostratigraphic data in addition to positions of tephra beds allow a preliminary thickness comparison of the lower two stratigraphic intervals. Here, we correlate strata based on the approxi-

TABLE 2. Tephra data for samples from upper, lower, and basal Rio del Oso stratigraphic sections and White ashes #2-3

Sample #	Location in strat sections *(informal name)*	date analyzed	SiO2	Al2O3	Fe2O3	MgO	MnO	CaO	TiO2	Na2O	K2O	Total
OC-189-271006-djk	Lower RDO, 105.0-106.6 m	1/17/2007	72.33	15.54	2.68	0.58	0.12	1.68	0.61	2.14	4.32	100.00
RDO-091106h-djk	Lower RDO: 101.9-102.0 m	12/4/2006	71.48	15.22	2.32	0.44	0.11	1.26	0.54	2.77	5.86	100.00
RDO-091106a-djk	Lower RDO: 100.6-100.9 m	1/17/2007	77.72	12.82	0.74	0.05	0.06	0.58	0.09	1.81	6.14	100.01
RDO-091106b-djk (pop2)	Lower RDO: 99.3 m	1/17/2007	72.78	15.22	2.54	0.28	0.11	0.93	0.34	2.14	5.66	100.00
RDO-091106b-djk (pop1)	Lower RDO: 99.3 m	1/17/2007	73.56	15.14	2.17	0.27	0.10	0.88	0.29	1.88	5.70	99.99
RDO-091106b-djk (total)	Lower RDO: 99.3 m	1/17/2007	73.04	15.19	2.42	0.28	0.11	0.92	0.32	2.05	5.67	100.00
OC-227-271006-FGA-djk[ς]	Upper RDO: 2.1-2.5	12/4/2006	77.03	12.67	0.84	0.05	0.05	0.57	0.10	2.31	6.39	100.00
RDO-091106c-djk[ς]	Lower RDO: 96.5-96.6 m	1/17/2007	76.99	12.87	0.84	0.07	0.04	0.57	0.10	2.19	6.33	100.00
RDO-091106g-djk (pop2)	Lower RDO: 89.9 m	1/17/2007	76.10	13.42	1.01	0.12	0.07	0.42	0.19	2.44	6.24	100.01
RDO-091106g-djk (pop1)	Lower RDO: 89.9 m	1/17/2007	77.68	12.70	0.73	0.07	0.06	0.53	0.12	2.02	6.09	100.00
RDO-091106g-djk (total)	Lower RDO: 89.9 m	1/17/2007	77.07	12.98	0.84	0.09	0.07	0.49	0.15	2.18	6.15	100.02
RDO-091106f-djk (pop1)	Lower RDO: 76.1-76.4 m	1/17/2007	75.88	13.14	2.72	0.07	0.14	0.51	0.25	1.59	5.71	100.01
RDO-091106f-djk (pop2)	Lower RDO: 76.1-76.4 m	1/17/2007	75.91	13.21	2.86	0.17	0.06	1.07	0.35	1.36	5.00	99.99
OC-188-271006-djk	Lower RDO: 27.9-28.0 m	12/4/2006	71.16	15.48	2.95	0.64	0.10	1.85	0.68	2.14	5.00	100.00
OC-187-011004-djk	11 m below top of basal RDO*	1/17/2007	77.60	12.73	0.87	0.07	0.06	0.56	0.12	1.74	6.24	99.99
OC-167-280904-djk (pop3)	Lower & basal RDO: 0 m	7/26/2006	75.84	12.95	4.06	0.06	0.16	1.22	0.33	1.11	4.27	100.00
OC-167-280904-djk (pop2)	*(basal gray fine marker ash)*	7/26/2006	77.09	12.62	3.35	0.03	0.08	0.96	0.28	1.16	4.44	0.85
OC-168-280904-djk	Basal RDO: -3.1 to -4.0 m *(basal white fine marker ash)*	1/17/2007	77.94	12.74	0.76	0.06	0.06	0.51	0.11	1.80	6.03	100.01
OC-186-011004-djk	Lower RDO: 1.8 m below base *(basal white fine marker ash)*	1/17/2007	77.98	12.76	0.70	0.06	0.06	0.50	0.10	1.93	5.92	100.01
WA2**	Base of SR-D, 42 m in SR-C	??	78.53	12.51	0.66	0.05	0.06	0.45	0.08	2.15	5.50	99.99
WA3**	17 m in SR-D, 62 m in SR-C	??	77.40	12.58	0.88	0.03	0.08	0.54	0.11	1.83	6.56	100.01

Notes:

* Ash collected 400 m south of strat section line

** Data for White Ashes #2 and #3 are from Borchert (2002). FeO recalculated to Fe2O3. Normalized to 100% on a water-free basis.

[ς] These two beds have a similarity coefficient of ~0.99 and are interpreted to be correlative.

mate middle of the Pojoaque white ash zone (PWAZ). In the upper Rio del Oso section, the thin bed of white ash that we correlate to the PWAZ is located about 20 m below eolian sediment of the Ojo Caliente Sandstone Member. This ash may correlate to two tephras in the Cuarteles section that are within 20 m of eolian sediment possibly correlative to the Ojo Caliente Sandstone Member; one tephra lies just below the base of unit 3i and the other is found in the upper part of unit 3k (Koning and Manley, 2003). Considering that the Pojoaque white ash zone is 100 m thick on the fault hanging wall and approximately 60-100 m thick on the footwall, we estimate the range of error in using the approximate middle of the Pojoaque white ash zone is less than 30 m (about 20-40 m of the PWAZ zone lies above the basal Ojo Caliente Sandstone Member contact in the Lyden quadrangle (Koning, 2004) and the ash bed in the upper Rio del Oso section is 20 m below the contact). Note that 30 m is less than the 80-105 m of thickness discrepancy in the stratigraphic interval corresponding to strata between the middle of the Pojoaque white ash zone and the top of the lower Barstovian tuffaceous zone (15.1-13.5 Ma). Thus, we infer that the SCF was active from 15.1 to 13.5 Ma. This fault activity seemed to have continued into the lower LCWAZ based on similar thickening index values for strata between the greenish dacite-bearing lapilli bed and the base of the LCWAZ.

Between the greenish dacite-bearing lapilli bed in the LCWAZ (~12.7 Ma) and the 10.0 to 9.4 Ma age datum, stratal accumulation rates decreased by roughly an order of magnitude and the hanging wall-normalized thickening index increased from ~40% to 75%. Although climatic changes may have reduced stratal accumulation rates across the entire basin, there is a significant difference in stratal thicknesses of this interval between the hanging wall and footwall sections. At this time, the Cuarteles section was experiencing alluvial slope deposition and the West Chili section was experiencing alternating axial river (Cejita Member, Chamita Formation) and distal piedmont deposition (Vallito Member)

TABLE 3. Comparison of similarity coefficients for White ashes #2-3 with lower Rio del Oso ashes.

Similarity coefficients (Na, Al, Si, K, Ca, Ti, Mn, Fe)*						**Similarity coeff. (Na, Al, Si, K , Ca, Fe)***					
	WA#3	**WA#2**	**OC-187**	**OC-168**	**OC-186**		**WA#3**	**WA#2**	**OC-187**	**OC-168**	**OC-186**
WA#3	1.0000	<0.91	0.9384 (**2**)	0.9302 (**3**)	<0.878	**WA#3**	1.0000	<0.905	0.9734 (**2**)	0.9486 (**4**)	0.9251 (**14**)
WA#2	<0.9002	1.0000	<0.9002	<0.9002	0.9304 (**3**)	**WA#2**	<0.914	1.0000	<0.914	0.9002	0.9405 (**3**)

Note:

* Relative similarity ranking of sample given in parenthesis (out of a total of 5548 tephra database entries, not including duplicate runs of the sample). Sample itself is given ranking of 1.

TABLE 4. Stratal accumulation rates and stratal thickening between footwall and hanging wall sections of the Santa Clara fault

Stratigraphic interval*	Height of lower contact (m)	Height of upper contact (m)	Thickness (m)	Approximate age of lower contact (Ma)	Approximate age of upper contact (Ma)	Stratal accumulation rate range (mm/yr)	Hanging wall-normalized thickening index**
9.4-10 Ma datum to dacite-bearing tephra of LCWAZ	6.8 (FW) 340.5 (HW)***	44.8 (FW) 558.3 (HW)***	38 (FW) 155 (HW)***	12.4-12.8	9.5-10	0.01 to 0.02 (FW) 0.05 to 0.06 (HW)	75%
Dacite-bearing tephra of LCWAZ to base of LCWAZ	-30 (FW) 280.5 (HW)	6.8 (FW) 340.5 (HW)	36.8 (FW) 60 (HW)	13.1	12.4-12.8	0.05 to 0.1 (FW) 0.09 to 0.2 (HW)	39%
middle of PWAZ to top of lower Barstovian tuff. interval	6.6 (FW) 116 (HW)[Ψ]	150 (FW) 106-130 (HW)[Ψ]	133-153 (FW)[ς] 237-261 (HW)[Ψ]	15.1	13.4-13.9	0.08 to 0.1 (FW) 0.1 to 0.2 (HW)	35 to 49%
lower Barstovian tuff. interval	-3.1 (FW) 0&42 (HW)[ω]	96.6 116&171 (HW)[ω]	100 (FW) 116 to 129 (HW)[ω]	15.1	15.4-15.8	0.1 to 0.3 (FW) 0.2 to 0.4 (HW)	16 to 22%

Notes:

* See text for more detail regarding stratigraphic interval: LCWAZ = lower coarse white ash zone; PWAZ = Pojoaque white ash zone.

** Index calculated by dividing the difference in stratal thickness between the hanging wall and footwall by the hanging wall thickness. Estimated error of ±15%.

*** upper contact is in Martinez section, and the lower contact in the middle Cuarteles section; thickness calculation considers the interpreted stratigraphic tie. between the two sections (i.e., that 505.6 m of the Martinez section correlates to 442.6m of the upper Cuarteles section)

Ψ upper contact is on lower Cuarteles section, and the lower contact is on the Skull Ridge section D; 85 m added to account for lower Pojoaque Member (Fig. 6)

ς +/- 10 m estimated error in correlating section across a fault

ω The two values are for Skull Ridge sections D and C, respectively

FW = footwall stratigraphic section (W Chili section and upper, lower, and basal Rio del Oso sections)

HW = hanging wall stratigraphic sections (Martinez, upper Cuarteles, middle Cuarteles, lower Cuarteles, and Skull Ridge sections)

from streams draining the Abiquiu embayment. In the absence of tectonic factors, the West Chili section might be expected to have higher stratal accumulation rates because it was closer to the axial river at this time, whereas the tributary streams of the Cuarteles Member (Tesuque Formation) would have lower stratal accumulation rates because of their greater distance from the axial river. The fact that we see the opposite trend argues for a strong tectonic signal, consistent with extension-related dike emplacement of the Chili dike swarm (Baldridge et al., 1980) and possibly the voluminous basalt eruptions near Cerro Roman and Lobato Mesa at 11.0 to 9.5 Ma. The increase in activity along the SCF with time may be due to linkage with the Pajarito fault system, or alternatively, perhaps regional extension rates increased after ~15.1 Ma and again after ~12.6 Ma.

It is noteworthy that the river depositing the Cejita Member shifted as much as 3 km westward onto the footwall block during deposition of the upper half of strata in the West Chili section (Fig. 6). Cejita Member deposits here appear to represent the axial river at this time because of their position in the basin and the lack of axial deposits in the Vallito Member. Paleocurrent data for the Cejita Member in the vicinity indicate southeast-south-southwest paleoflow (Koning et al., 2005a), and one can map this same unit under the basalt flows capping Black Mesa to the north (Koning and Manley, 2003), where it overlies a thick bed of fine white ash chemically correlated to a 11.3 Ma Trapper Creek ash (Koning, 2004). Considering the 10.11 Ma ± 0.07 Ma age (Maldonado and Miggins, 2007) of the capping basalt flow in the west Chili section, this westward onlapping of the axial river occurred between 11 and 10 Ma. Perhaps movement on the SCF slowed during this time so that the axial river was not constrained to the actively subsiding hanging wall of the fault and shifted westwards. Alternatively, sediment supply for the Cejita Member fluvial system may have increased significantly at that time.

That the SCF was undergoing normal throw in the middle Miocene is not unexpected. Koning et al. (2005b) demonstrated active westward tilting in the Española Basin during middle Miocene time, so it is reasonable to assume that the SCF would accommodate a component of normal movement. Also, Koning et al. (2004a) interpreted motion along the Velarde fault in the early to middle Miocene based on seismic reflection data. The southern Pajarito fault was active in the Oligocene or early Miocene through the middle Miocene based on an angular unconformity underlying a condensed basin-fill section on the footwall of the fault at St. Peter's Dome (Gardner et al., 1986; Goff et al., 1990; Cather, 1992; Smith, 2004). Lastly, correlations between wells in the Guaje well field, located 6-7 km north-northeast of Los Alamos, indicate throw along faults between 13.2 and 11.6 Ma (WoldeGabriel et al., 2006).

An increase in vertical fault motion beginning around 12.7 Ma is consistent with the general geology and sedimentologic features on the SCF footwall. In particular, the Ojo Caliente Sandstone Member (13.4-12.5 Ma) varies in thickness from 0 to 360 m under the 11 to 9.5 Ma Lobato Formation basalts near and north of Cerro Roman (Figs. 2, 5; Koning et al., 2005b). Significant throw on the Santa Clara and other local faults between the initiation of Ojo Caliente Sandstone Member deposition and the emplacement of Lobato Formation basalts is required to account for this thickness variation. The fact that the Ojo Caliente Sandstone Member is about 100 m thick 2 km north of lower Santa Clara Creek (Koning, 2002) and extends east of the Rio Grande makes it unlikely that the thickness variations in the Cerro Roman area are due to thinning at the edge of the Ojo Caliente dune field. In the Vallito Member, sandy sediment of 12.7 to 10.0 Ma age generally lack sedimentary structures (suggesting more time for bioturbation) and have relatively abundant paleosols (particularly in the West Chili section), consistent with slower aggradation rates on a relatively uplifted footwall block.

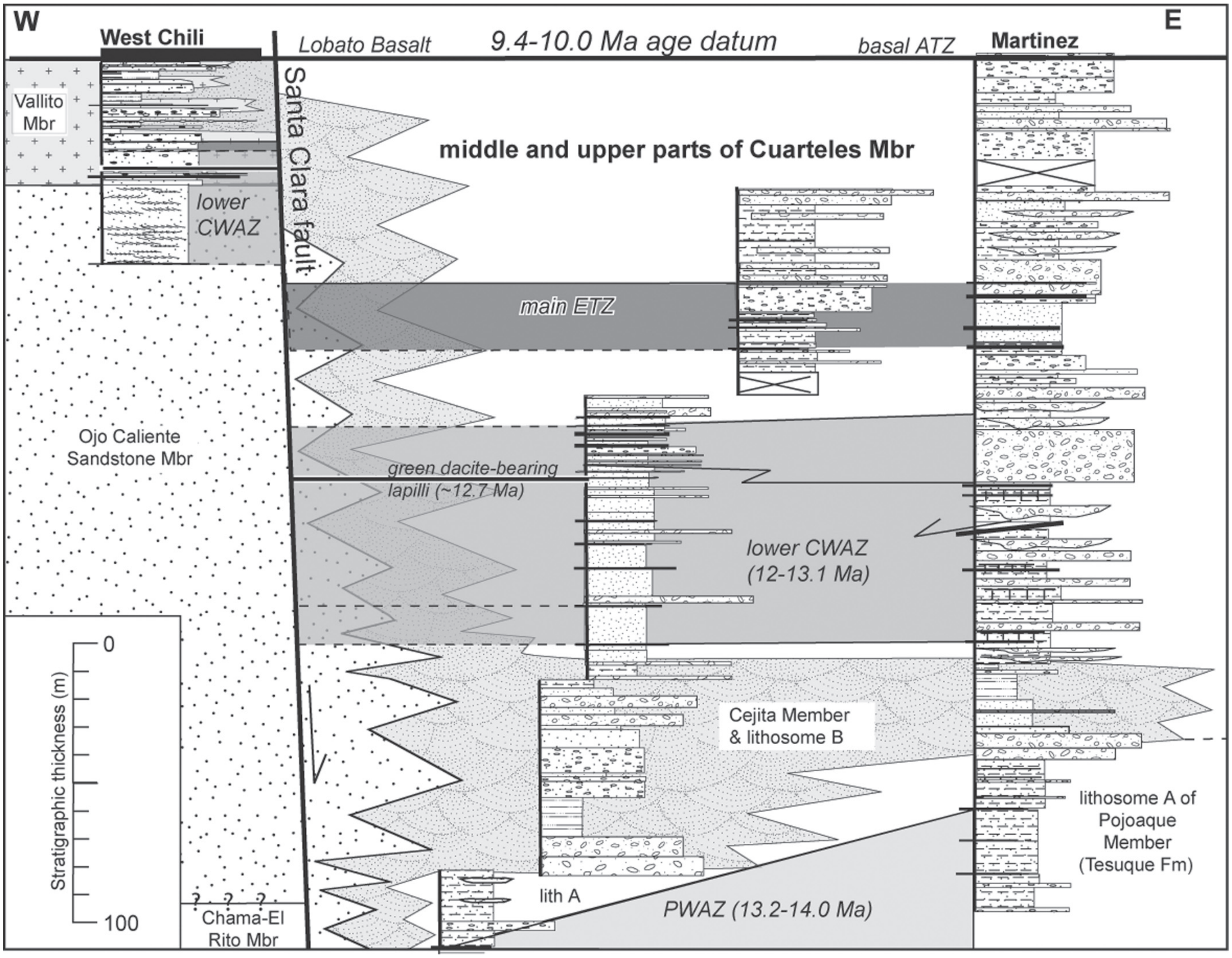

FIGURE 8. West-east stratigraphic fence diagram illustrating our correlations between middle to upper Miocene footwall and hanging-wall strata west and east of Española. The graphic patterns between the individual stratigraphic sections show the relative extents and positions of the Vallito Member (Chamita Formation), Ojo Caliente Sandstone Member (Tesuque Formation), and Cejita Member (Tesuque and Chamita Formations). Thickness of Ojo Caliente Sandstone Member is from Koning et al. (2005b, fig. 7). The Cuarteles Member and lithosome A of the Pojoaque Member (Tesuque Formation) is unshaded.

The SCF continued to experience normal throw through the late Miocene and Pliocene. For example, the cross-section of figure 1.13 in the 1st Day Roadlog suggests 430-500 m of stratigraphic separation of the 12.4-9.5 Ma phreatomagmatic deposit discussed earlier. The SCF and Puye faults together have produced a cumulative vertical offset of at least 60 m of the upper surface of the Puye Formation, based on estimating fault scarp heights from the geologic map of Koning et al. (2005b). The fact that few post-10 Ma strata are preserved on the footwall of the SCF is consistent with relatively large amounts of throw during the late Miocene and Pliocene.

CONCLUSIONS

This study extends the middle Miocene tectonic investigation undertaken by Koning et al. (2005b) by comparing stratal thickness differences on either side of the SCF for middle to upper Miocene strata. Further efforts at this correlation are ongoing for the lowest interval (lower middle Miocene). A preliminary comparison of the thickness of the entire lower Barstovian tuffaceous zone suggests a slight thickening of strata across the SCF during this time (16-22% hanging wall-normalized thickening index). Differences in stratal thicknesses (25-49% thickening index) between the approximate middle Pojoaque white ash zone and the top of the lower Barstovian tuffaceous zone suggests significant motion along the fault between ~15.1 and 13.5 Ma. A short interval at the base of the lower coarse white ash zone suggests vertical slip rates during 13.1 to 12.7 Ma were similar to ~15.1 - 13.5 Ma rates. Vertical slip rates increased between 12.7 and 10.0 Ma because hanging-wall strata of this age became significantly thicker compared to footwall strata (75% thickening index), and the thickness of Ojo Caliente Sandstone Member under ~10 Ma

Lobato basalt flows varies from 0 to 360 m in the vicinity of Cerro Roman. The axial river migrated 3 km onto the footwall of the fault during 11-10 Ma, indicating either a brief decrease in vertical slip rates or an increase in this river's sedimentation rate. Vertical slip rates remained relatively high after 10 Ma because of the general lack of preservation of strata of that age on the fault footwall; also, there is 430 to 500 m of interpreted throw along the SCF since emplacement of 12.5-9.5 Ma phreatomagmatic deposits.

ACKOWLEDGMENTS

We thank our reviewers Steve Cather and David Dethier. Funding for the field geologic work was provided by the STATEMAP program. We thank David B. Wahl for helping to analyze the tephra samples, and especially appreciate the interpretations and judgments of Andrei Sarna-Wojcicki regarding our tephra samples. The analytical work by the USGS Tephrochronology Laboratory is funded by the National Cooperative Geologic Mapping Program.

REFERENCES

Aldrich, M.J. Jr., 1986, Tectonics of the Jemez lineament in the Jemez Mountains and Rio Grande rift: Journal of Geophysical Research, vol. 91, no. B2, p. 1753-1762.

Aldrich, M.J., and Dethier, D.P., 1990, Stratigraphic and tectonic evolution of the northern Española Basin, Rio Grande rift, New Mexico: Geological Society of America Bulletin, v. 102, p. 1695-1705.

Baldridge, W.S., Damon, P.E., Shafiqullah, M., and Bridwell, R.J., 1980, Evolution of the central Rio Grande rift, New Mexico – new Potassium-Argon ages: Earth and Planetary Science Letters, v. 51, p. 309-321.

Baldridge, W.S., Ferguson, J.F., Braile, L.W., Wang, B., Eckhardt, K., Evans, D., Schultz, C., Gilpin, B., Jiracek, G., and Biehler, S., 1994, The western margin of the Rio Grande rift in northern New Mexico: an aborted boundary?: Geological Society of America Bulletin, v. 105, p. 1538-1551.

Baltz, E.H., 1978, Resume of Rio Grande depression in north-central New Mexico: New Mexico Bureau of Mines and Mineral Resources, Circular 163, p. 210-228.

Barghoorn, S., 1981, Magnetic-polarity stratigraphy of the Miocene type Tesuque Formation, Santa Fe Group, in the Española Valley, New Mexico: Geological Society of America Bulletin, v. 92, p. 1027-1041.

Borchert, C., 2002, Geology and ground-water flow, Tesuque quadrangle, Santa Fe County, New Mexico [M.S. thesis]: Albuquerque, University of New Mexico, 129 p.

Brown, L.L., and Golombek, M. P., 1985, Tectonic rotations within the Rio Grande rift: evidence from paleomagnetic studies: Journal of Geophysical Research, vol. 90, no. B1, p. 790-802.

Cande, S.C., and Kent, D.V., 1995, Revised calibration of the geomagnetic polarity timescale for the Late Cretaceous and Cenozoic: Journal of Geophysical Research, v. 100, no. B4, p. 6093-6095.

Cather, S.M., 1992, Suggested revisions to the Tertiary tectonic history of north-central New Mexico: New Mexico Geological Society, 43th Field Conference, Guidebook, p. 109-122.

Cavazza, W., 1986, Miocene sediment dispersal in the central Española Basin, Rio Grande rift, New Mexico, USA: Sedimentary Geology, v. 51, p. 119-135.

Cordell, L., 1979, Gravimetric expression of graben faulting in Santa Fe country and the Española Basin, New Mexico: New Mexico Geological Society, 30th Field Conference, Guidebook, p. 59-64.

Dethier, D.P., and Manley, K., 1985, Geologic map of the Chili quadrangle, Rio Arriba County, New Mexico: United States Geological Survey, Miscellaneous Field Studies Map MF-1814, scale 1:24000.

Dethier, D.P., and Martin, B.A., 1984, Geology and structure along part of the northeast Jemez Mountains, New Mexico: New Mexico Geological Society, 35th Fiield Conference, Guidebook, p. 145-150.

Dethier, D.P., Aldrich, M.J. Jr., and Shafiqullah, M., 1986, New K-Ar ages for Miocene volcanic rocks from the northeastern Jemez Mountains and Tejana Mesa, New Mexico: Isochron/West, no. 47, p. 12-14.

Ekas, L.M., Ingersoll, R.V., Baldridge, W.S., and Shafiqullah, M., 1984, The Chama-El Rito Member of the Tesuque Formation, Española Basin, New Mexico: New Mexico Geological Society Guidebook, 35th Field Conference, Guidebook, p. 137-143.

Ferguson, J.F., Baldridge, W.S., Braile, L.W., Biehler, S., Gilpin, B., and Jiracek, G., 1995, Structure of the Española Basin, Rio Grande rift, New Mexico, from SAGE seismic and gravity data: New Mexico Geological Society, 46th Field Conference, Guidebook, p. 105-110.

Galusha, T., and Blick, J.C., 1971, Stratigraphy of the Santa Fe Group, New Mexico: Bulletin of the American Museum of Natural History, v. 144, 127 p.

Gardner, J.N., Goff, F., Garcia, S., and Hagan, R.C., 1986, Stratigraphic relations and lithologic variations in the Jemez volcanic field: Journal of Geophysical Research, v. 91, p. 1763-1778.

Goff, F., Gardner, J., Baldridge, W., Hulen, J., Nielsen, D., Vaniman, D., Heiken, G., Dungan, M., and Broxton, D., 1989, Excursion 17B: volcanic and hydrothermal evolution of the Valles caldera and Jemez volcanic field: New Mexico Bureau of Mines and Mineral Resources, Memoir 46, p. 381-434.

Goff, F., Gardner, J.N., and Valentine, G.A., 1990, Geology of St. Peter's Dome area, Jemez Mountains, New Mexico: New Mexico Bureau of Mines and Mineral Resources, Geologic Map 69, scale 1:24,000.

Golombek, M.P., 1983, Geology, structure, and tectonics of the Pajarito fault zone in the Española Basin of the Rio Grande rift, New Mexico: Geological Society of America Bulletin, v. 94, p. 192-205.

Gonzalez, M.A., 1993, Geomorphic and neotectonic analysis along a margin of the Colorado Plateau and Rio Grande rift in northern New Mexico [Ph.D. dissertation]: Albuquerque, University of New Mexico, 302 p.

Harrington, C.D., and Aldrich, M.L. Jr., 1984, Development and deformation of Quaternary surfaces on the northeastern flank of the Jemez Mountains: New Mexico Geological Society, 35th Field Conference, Guidebook, p. 235-239.

Izett, G.A., and Obradovich, J.D., 2001, 40Ar/39Ar ages of Miocene tuffs in basin-fill deposits (Santa Fe Group, New Mexico, and Troublesome Formation, Colorado) of the Rio Grande rift system: The Mountain Geologist, v. 38, p. 77-86.

Johnpeer, G., D., Love, D.W., Hawley, J.W., Bobrow, D.J., Hemingway, M., and Reimers, R.F., 1985, El Llano and vicinity geotechnical study: unpublished report for the Office of Military Affairs, Santa Fe, NM.

Justet, L., 2003, Effects of basalt intrusion on the multi-phase evolution of the Jemez volcanic field, NM [Ph.D. dissertation]: Las Vegas, University of Nevada, 248 p.

Kelley, V.C., 1978, Geology of the Española Basin, New Mexico: New Mexico Bureau of Mines and Mineral Resources, Geologic Map 48, scale 1:125,000.

Kelley, V.C., 1979, Tectonics, middle Rio Grande rift, New Mexico, *in* Riecker, R.E., ed., Rio Grande rift: tectonics and magmatism: Washington, D.C., American Geophysical Union, p. 71-86.

Kelson, K.I., Bauer, P.W., Unruh, J.R., and Bott, J.D.J., 2004, Late Quaternary characteristics of the northern Embudo fault, Taos County, New Mexico: New Mexico Geological Society, 55th Field Conference, Guidebook, p. 147-157.

Koning, D.J., 2002, Geology of the Española 7.5-minute quadrangle and implications regarding middle Miocene deposition and tectonism in the Rio Grande rift, north-central New Mexico (abs.): New Mexico Geology, v. 42, p. 63.

Koning, D.J., 2003, revised Dec-2005, Geologic map of the Chimayo 7.5-minute quadrangle, Rio Arriba and Santa Fe Counties, New Mexico: New Mexico Bureau of Geology and Mineral Resources, Open-file Geologic Map OF-GM-71, scale 1:24,000.

Koning, D.J., 2004, Geologic map of the Lyden 7.5-minute quadrangle, Rio Arriba and Santa Fe Counties, New Mexico: New Mexico Bureau of Geology and Mineral Resources, Open-file Geologic Map OF-GM-83, scale 1:24,000.

Koning, D.J., and Aby, S., 2003, revised June-2004, Geologic map of the Velarde 7.5-minute quadrangle, Rio Arriba and Taos Counties, New Mexico: New Mexico Bureau of Geology and Mineral Resources, Open-file Geologic Map OF-GM-79, scale 1:24,000.

Koning, D.J., and Aby, S., 2005, Proposed members of the Chamita Formation,

north-central New Mexico: New Mexico Geological Society, 56th Field Conference, Guidebook, p. 258-278.
Koning, D.J., and Manley, K., 2003, revised Dec-2005, Geologic map of the San Juan Pueblo 7.5-minute quadrangle, Rio Arriba and Santa Fe Counties, New Mexico: New Mexico Bureau of Geology and Mineral Resources, Open-file Geologic Map OF-GM-70, scale 1:24,000.
Koning, D.J., Nyman, M., Horning, R., Eppes, M., and Rogers, S., 2002, Geology of the Cundiyo 7.5-min. quadrangle, Santa Fe County, New Mexico, New Mexico Bureau of Geology and Mineral Resources, Open-file Geologic Map OF-GM-56, scale 1:24,000.
Koning, D.J., Ferguson, J.F., Paul, P.J., and Baldridge, W.S., 2004a, Geologic structure of the Velarde graben and southern Embudo fault system, north-central N.M.: New Mexico Geological Society, 55th Field Conference, Guidebook, p. 158-171.
Koning, D.J., Aby, S.B., and Dunbar, N., 2004b, Middle-upper Miocene stratigraphy of the Velarde graben, north-central New Mexico: tectonic and paleogeographic implications: New Mexico Geological Society, 55th Field Conference, Guidebook, p. 359-373.
Koning, D., May, J., Aby, S., and Horning, R., 2004c, Geologic map of the Medanales 7.5-minute quadrangle, Rio Arriba county, New Mexico: New Mexico Bureau of Geology and Mineral Resources, Open-file Geologic Map OF-GM-89, scale 1:24,000.
Koning, D.J., Skotnicki, S., Moore, J., and Kelley, S., 2005a, Geologic map of the Chili 7.5-minute quadrangle, Rio Arriba County, New Mexico: New Mexico Bureau of Geology and Mineral Resources, Open-file Geologic Map OF-GM-81, scale 1:24,000.
Koning, D.J., Connell, S.D., Morgan, G.S., Peters, L., and McIntosh, W.C., 2005b, Stratigraphy and depositional trends in the Santa Fe Group near Española, north-central New Mexico: tectonic and climatic implications: New Mexico Geological Society, 56th Field Conference, Guidebook, p. 237-257.
Koning, D.J., Kelley, S.A., and Kempter, K. A., 2007, Geologic sructures near teh boundary of the Abiquiu embayment and Colorado Plateau - a long history of faulting: New Mexico Geological Society, 58th Field Conference, Guidebook, p. 43-46.
Kuhle, A., 1997, Sedimentology of Miocene alluvial-slope deposits, Española Basin, Rio Grande rift: an outcrop analogue for subsurface heterogeneity [M.S. thesis]: Albuquerque, University of New Mexico, 205 p.
Kuhle, A., and Smith, G.A., 2001, Alluvial-slope deposition of the Skull Ridge Member of the Tesuque Formation, Española Basin, New Mexico: New Mexico Geology, p. 30-37.
Machette, M.N., Personius, S.F., Kelson, K.I., Haller, K.M., and Dart, R.L., 1998, Map and data for Quaternary faults in New Mexico: U.S. Geological Survey, Open-file Report 98-521, 443 p.
Maldonado, F., and Miggins, D.P., 2007, Geologic summary of the Abiquiu quadrangle, north-central New Mexico: New Mexico Geological Society, 58th Field Conference, Guidebook, p.182-187.
Manley, K., 1976, The late Cenozoic history of the Española Basin, New Mexico [Ph.D. dissertation]: Boulder, University of Colorado, 171 p.
Manley, K., 1977, Geologic map of the Cejita Member (new name) of the Tesuque Formation, Española Basin, New Mexico: U.S. Geological Survey, Miscellaneous Field Studies Map MF-877, scale 1:24000.
Manley, K., 1979, Tertiary and Quaternary stratigraphy of the Northeast Plateau, Española Basin, New Mexico: New Mexico Geological Society, 30th Field Conference, Guidebook, p. 231-236.
May, J., 1980, Neogene geology of the Ojo Caliente-Rio Chama area, Española Basin, New Mexico [Ph.D. dissertation]: Albuquerque, University of New Mexico, 204 p.
May, J., 1984, Miocene stratigraphic relations and problems between the Abiquiu, Los Pinos, and Tesuque formations near Ojo Caliente, northern Española Basin: New Mexico Geological Society, 35th Field Conference, Guidebook, p. 129-135.
Moore, J.D., 2000, Tectonics and volcanism during deposition of the Oligocene-lower Miocene Abiquiu Formation in northern New Mexico [M.S. thesis]: Albuquerque, University of new Mexico, 147 p.
Muehlberger, W.R., 1979, The Embudo fault between Pilar and Arroyo Hondo, New Mexico: an active intracontinental transform fault: New Mexico Geological Society, 30th Field Conference, Guidebook, 77-82.
North American Commission on Stratigraphic Nomenclature [NACSN], 2005, North American stratigraphic code: American Association of Petroleum Geologists Bulletin, v. 89, p. 1547-1591.
Salyards, S.,L., Ni, J.F., and Aldrich, M.J. Jr., 1994, Variation in paleomagnetic rotations and kinematics of the north-central Rio Grande rift, New Mexico: Geological Society of America, Special Paper 291, p. 59-71.
Smith, G.A., 2004, Middle to late Cenozoic development of the Rio Grande rift and adjacent regions in northern New Mexico, *in* Mack, G.H., and Giles, K.A., eds., The geology of New Mexico, a geologic history: New Mexico Geological Society, Special Publication 11, p. 331-358.
Smith, G.A., Moore, J.D., and McIntosh, W.C., 2002, Assessing roles of volcanism and basin subsidence in causing Oligocene-lower Miocene sedimentation in the northern Rio Grande rift, new Mexico: Journal of Sedimentary Research, v. 72, p. 836-848.
Spiegel, Z., and Baldwin, B., 1963, Geology and water resources of the Santa Fe area, New Mexico: U.S. Geological Survey, Water-Supply Paper 1525, 258 p.
Steinpress, M.G., 1980, Neogene stratigraphy and structure of the Dixon area, Española Basin, north-central New Mexico [M.S. thesis]: Albuquerque, University of New Mexico, 127 p.
Steinpress, M.G., 1981, Neogene stratigraphy and structure of the Dixon area, Española Basin, north-central New Mexico: Geological Society of America Bulletin, Part II, v. 92, no. 12, p. 2553-2671.
Tedford, R.H., and Barghoorn, S.F., 1993, Neogene stratigraphy and mammalian biochronology of the Española Basin, northern New Mexico: New Mexico Museum of Natural History and Science, Bulletin 2, p. 159-168.
Tedford, R. H., Albright, L.B. III, Barnosky, A.D., Ferrusquia-Villafranca, I., Hunt, L.M. Jr., Storer, J.E., Swisher, C.C. III, Voorhies, M.R., Webb, S.D., and Whistler, D.P., 2004, Mammalian biochronology of the Arikareean through Hemphillian interval (late Oligocene through early Pliocene epochs), *in* Woodburne, M.O.,ed., Late Cretaceous and Cenozoic mammals of North America: biostratigraphy and geochronology: New York, Columbia University Press, p. 169-231.
WoldeGabriel, G., Warren, R.G., Chipera, S., and Keating, E., 2006, Geological characteristics of the Guaje well field of the Pajarito Plateau in the Española Basin, Rio Grande rift: Oak Ridge, U.S. Department of Energy, report LA-UR-06-2438, 65 p.

PLATE 10: GEOLOGIC MAP OF THE CHILI 7.5-MINUTE QUADRANGLE, NM

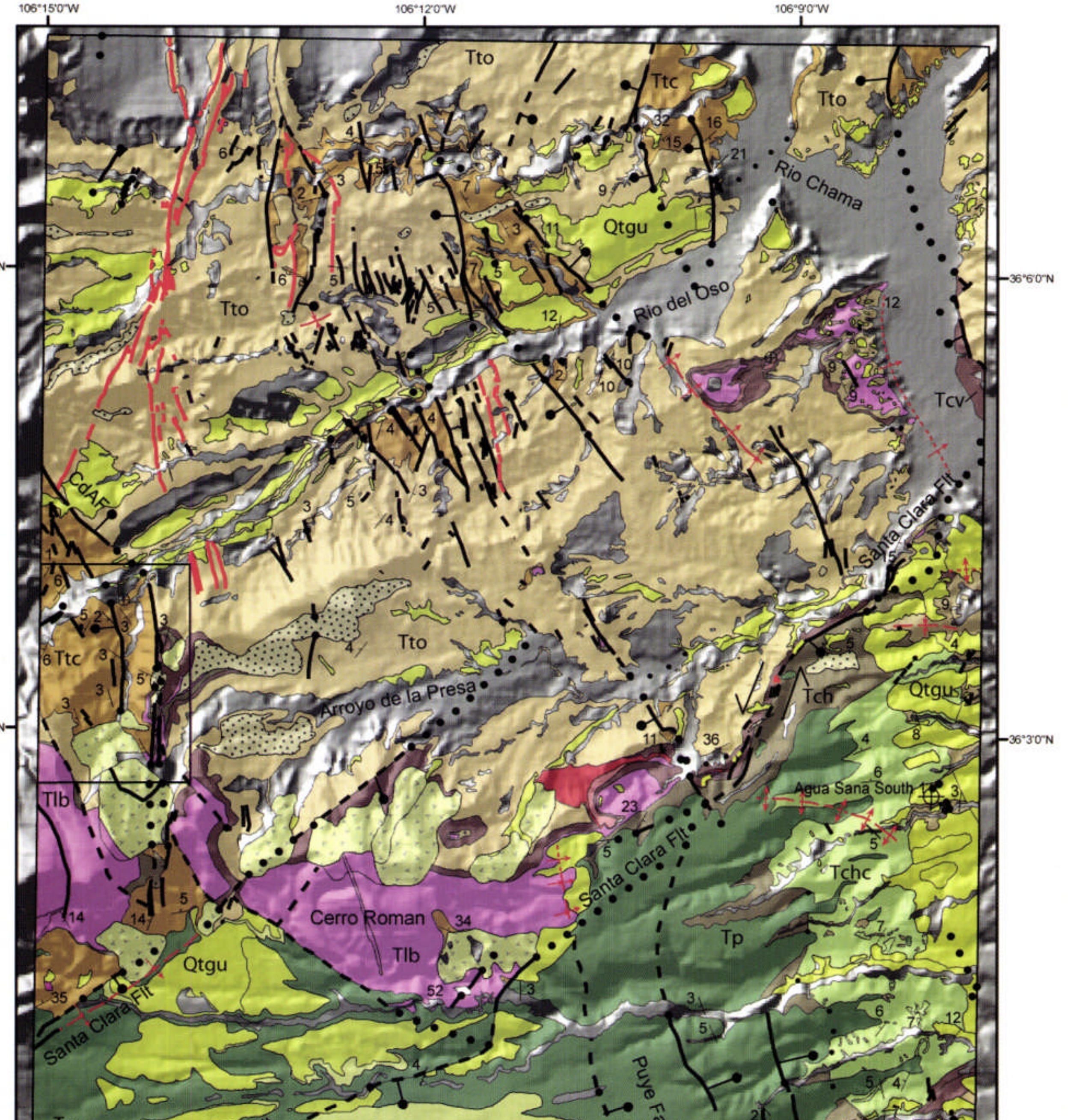

Geologic map of the Chili 7.5-minute quadrangle (Koning et al., 2005a). Rectangular box along west margin is location of map shown in Figure 1.73 of the minipaper by Koning and Kempter on page 50. CdAF = Canada del Almagre fault. Quaternary valley-fill units not shown. See article by Koning et al. on page 225.